J Solid State Electrochem (2011) 15:877–890
DOI 10.1007/s10008-011-1324-9

REVIEW

The use of in situ techniques in R&D of Li and Mg rechargeable batteries

S. Francis Amalraj · Doron Aurbach

Received: 25 January 2011 / Accepted: 28 January 2011 / Published online: 22 February 2011

Abstract Rechargeable batteries are complicated devices in which three bulk zones (electrodes, electrolyte solution) and two interfaces have to work simultaneously and coherently, without any side reactions. The study of electrode materials and electrode–solution interfaces of rechargeable batteries requires the use of first-rate techniques for structure and surface analysis, in conjunction with electrochemical methods. The use of in situ techniques in which spectroscopy, diffractometry, or microscopy are measured in conjunction with an electrochemical response may be highly important and beneficial for battery research. We review herein the use of in situ Fourier transform–infrared spectroscopy, Raman, X-ray absorption, mass spectrometry, X-ray diffraction, atomic force microscopy, scanning tunneling microscopy, and electrochemical quartz crystal microbalance techniques for research and development of rechargeable Li and Mg batteries.

Keywords In situ techniques · Rechargeable Li and Mg batteries · Surface analysis · Electrochemical systems

Introduction

R&D of rechargeable batteries requires rigorous work in materials and surface science. Since an obvious need from rechargeable batteries is high energy density, we have to use highly reactive materials for their electrodes. As the anode materials, the natural selection is the use of the most reactive and light metals, lithium and magnesium. Li reacts readily with all atmospheric components (N_2, O_2, H_2O, and CO_2) except noble gases and with all protic and polar aprotic solvents [1]. Magnesium also reacts with active atmospheric components (obviously with CO_2 and H_2O), protic solvents, and several reactive aprotic solvents (e.g., alkyl carbonates) [2]. Magnesium's lower reactivity, compared to lithium, keeps it stable in ether solvents [3]. The reactions of both Li and Mg with atmospheric and solution species form insoluble reduction products that are mostly salts of the active materials [4]. Hence, both Li and Mg electrodes are surface film controlled. In the case of lithium, surface films comprising Li salts are always Li-ion conductive, under an electrical field. Hence, surface films on Li electrodes can be considered as a solid electrolyte interphase [5]. Hence, when Li electrodes are operated, Li-ion deposition and dissolution processes involve the obvious step of Li-ion migration through surface films. The surface films formed on lithium in any polar aprotic solution comprise a variety of possible surface species because solvent molecules, salt anions and impurities (e.g., trace water), are reduced simultaneously by the active metal. Moreover, Li metal is always introduced into solutions while being covered by native surface films. Thus, the partial replacement of the native film by the new surface compounds takes place. Hence, the surface films on Li are very heterogeneous, and thereby, the current distribution of Li dissolution/deposition is never uniform. This leads to non-uniform dendrite formation upon Li deposition and to morphological complications that prevent the possibility of using Li-metal anodes in rechargeable Li batteries [6, 7].

The replacement of Li metal by a graphite-intercalation compound as the anode material in rechargeable Li batteries led to the revolutionary development of Li-ion batteries [8]. In these systems, the Li source comes from the cathode

S. F. Amalraj · D. Aurbach (✉)
Department of Chemistry, Bar-Ilan University,
Ramat-Gan 52900, Israel
e-mail: aurbach@mail.biu.ac.il

side, whose active mass is usually a lithiated transition metal oxide. The first process in Li-ion batteries is charging, in which graphite electrodes are polarized cathodically down to Li-ion insertion potentials (0.25–0.01 V vs. Li/Li^+). Components of polar aprotic solvents are reduced on noble metal electrodes at potentials lower than 2 V (Li/Li^+) in the following order: HF <1.8 V, trace water 1.5 V, alkyl carbonates <1.5 V, esters <1 V, ethers <0.5 V, and salt anions such as PF_6^-, ClO_4^-, and BF_4^- <1 V [9]. It should be noted that these reduction processes and their onset potentials are highly influenced by the nature of the cation. In the presence of Li ions in solutions, all the above reduction processes in polar aprotic solvents produce surface films similar in their basic chemistry to that of Li metal in the same solutions [10]. Hence, the polarization of graphite electrodes to potentials below 1.5 V vs. Li/Li^+ induces electro-reduction processes on their surfaces. These form insoluble Li salts that precipitate on the graphite electrodes to form Li-ion conducting surface films. It should be noted that graphite has a very fragile structure. Solvent molecules attached to the Li ions (their salvation shell) can co-intercalate into the graphite structure with the Li ions [11]. This co-intercalation process is very detrimental. The solvent molecules can be reduced within the graphite structure, and hence, graphite particles can exfoliate, and are destroyed [12]. Therefore, the quick formation of passivating protective surface films on graphite electrodes before detrimental co-intercalation and exfoliation processes take place is critical to the operation of Li-inserted graphite electrodes as reversible anodes in Li-ion batteries [12]. Hence, both Li and graphite electrodes require a rigorous study of the correlation among surface chemistry, morphology, and their electrochemical response, in order to promote their use in batteries.

It should be noted that Li_xMO_y-lithiated transition metal cathodes also develop rich surface chemistry in polar aprotic solutions [13]. Their surface chemistry definitely determines their performance. It can be said that in Li-ion batteries neither the anodes nor the cathodes maintain thermodynamic stability in most relevant polar aprotic solvents. This situation motivates very strongly the basic R&D of these systems on a comprehensive understanding of the impact of morphology and surface chemistry of the active mass on the electrochemical performance. The situation with Mg electrodes is quite different to that of Li and Li-ion electrodes. Surface films comprising Mg salts cannot conduct the bivalent Mg ions [2]. Therefore, whenever Mg electrodes are covered by surface films, Mg dissolution may take place only at very high overpotentials via the break-and-repair of the surface films, while Mg deposition is impossible. Hence, Mg electrodes can behave reversibly only when they are bare (no surface films at all), Mg electrodes behave reversibly with Grignard reagents (RMgX; X = Cl, Br; R = alkyl or aryl groups) or with complex reagents of the $Mg(BR_4)_2$ and $Mg(AlCl_{4-n}R_n)_2$ type [14]. Mg deposition and dissolution processes in these solutions are complicated by adsorption phenomena [15]. In order to develop battery systems based on Li, Li-graphite, or Mg electrodes, it is important to understand as thoroughly as possible the interactions between active electrodes and polar aprotic electrolyte solutions. It is then possible to adjust the Li or Mg battery systems to relevant electrolyte solutions.

Due to the high reactivity of Li, Mg, or Li-C electrodes with atmospheric gases, their ex situ surface analysis may not be authentic, because as the electrodes are removed from the solutions, they can readily react with trace O_2, N_2, H_2O, CO_2, etc. Thereby, it was critically important to use in situ spectroscopic and microscopic measurements in which the surface chemistry and morphology of the reactive electrodes can be studied in solutions, under potential control. In this review, we described relevant in situ techniques that were developed for highly reactive electrochemical systems: Li, Mg, Li-C, and Li-insertion electrodes of the Li_xMO_y type (M = transition metal, single or a mixture, including Co, Ni, Mn, Fe, and V) in polar aprotic solutions.

In the next section, a wide variety of in situ techniques used in battery research are briefly reviewed. In the last section, we emphasize work related to Li, Li-graphite, and Mg electrodes that can be considered as among the most reactive (yet meta-stable) electrochemical systems. We demonstrate herein the importance of in situ techniques for the study of such reactive systems.

In situ techniques relevant for battery research

Spectroscopic tools

The various analytical techniques that are used in situ, in conjunction with electrochemical measurements, can be divided into several categories:

1. Surface sensitive vs. bulk techniques
2. Spectroscopic, microscopic, and diffractometric tools

The main spectroscopic techniques used in battery research include Fourier transform–infrared spectroscopy (FTIR) [16], Raman [17], solid-state nuclear magnetic resonance (NMR) [18], mass spectrometry (MS) [19], and methods based on X-ray spectroscopy: X-ray absorption near edge structure (XANES), and extended X-ray absorption fine structure (EXAFS) [20]. From these tools, only FTIR can be considered as a surface sensitive technique. Raman spectroscopy can be considered as a surface sensitive technique only if the surface layers are thick enough, or due to the special morphology of the electrode

surface, when an enhancement of the response is obtained [21] (termed as surface enhanced Raman spectroscopy, and it is beyond the scope of this review). However, in general, due to the relatively weak signal of the Raman spectra, it should be considered as a bulk technique.

Solid-state NMR is highly useful for the study of Li intercalation processes, concentrating on the ^{6}Li and ^{7}Li nuclei [22, 23]. Working with other nuclei such as ^{1}H, ^{19}F, ^{31}P, ^{13}C, and ^{27}Al may also be relevant [24]. The use of SS NMR as an in situ tool was demonstrated recently for the complicated process of silicon lithiation and the possible use of high-capacity Li-Si anodes for Li-ion batteries (4.4 Li + Si ⇌ $Li_{4.4}Si$, capacity around 4,000 mAh/g). The use of this technique, in situ, was proven as highly important for the analysis of meta-stable phases that are termed Li-Si [25].

Mass spectrometry was used as a tool for the study of volatile products formed by interfacial reactions between Li-graphite anodes and selected electrolyte solutions (mostly alkyl carbonates) [26]. The electrochemical cells for these measurements are connected to the high vacuum systems of the mass spectrometer, via a porous ceramic membrane that prevents the transport of solutions species to the system, but allows the migration of volatile products from the electrochemical cell to the spectrometer. These methods can monitor the potential-dependent formation of gaseous products, due to solutions reduction upon the cathodic polarization of graphite electrodes[27].

Spectroscopic techniques based on X-ray absorption, XANES, and EXAFS are being increasingly used in battery research [28, 29]. It is possible to follow in situ changes in the electronic environment of key elements in electrode materials by XANES [30], and to follow in situ changes in the inter-atomic distances between atoms of electrode materials by EXAFS, during the operation of full Li batteries [31]. For the use of these techniques, a synchrotron X-ray source is needed in order to have an X-ray beam with a high enough power density for a clear response (a high enough signal-to-noise ratio). Hence, such measurements have to be carried out only in research centers that possess synchrotron systems. It is possible to design full batteries that can be cycled while being under the culminated X-ray beam, in a way that only one of the components (usually the cathode) dominates the response to the X-ray absorbance. These techniques are extremely useful for the study of new Li-insertion cathode materials [32].

Electrochemical quartz crystal microbalance

Electrochemical quartz crystal microbalance (EQCM) can be considered as an in situ surface sensitive technique that is complementary to the use of an in situ tool such as FTIR. It is based on the piezo-electric response of thin quartz crystals whose vibration is affected by possible surface loads. The behavior that allows the use of thin quartz crystals as analytical tools relates to the Sauerbrey equation: Δf=constant x, which sets a linear relationship between changes in mass loads on the thin crystal (Δm) and the natural frequency of the crystal (Δf), provided that there are no visco-elastic effects that perturb this linear response [33]. Hence, as was demonstrated in many publications, it is possible to fabricate working metallic electrodes (Au, Pt) deposited on quartz crystals whose electrochemical response in three-electrode cells is measured together with changes in the frequency response of the quartz crystal, due to the electrochemical processes that the working electrode (thin metallic film on the quartz crystal) undergoes [34–36].

The frequency measurements are translated to mass changes in electrodeposition–dissolution processes [37], surface film formation [38], and adsorption processes [39]. Since both Δm and the charge involved are measured, it is possible to calculate the mass per electron (m.p.e) values for various electrochemical processes measured by EQCM and compare these values to equivalent weights of possible surface species that are deposited or dissolved [38, 40]. EQCM was extensively used for the study of electrodeposition processes, electro-adsorption phenomena, and transport phenomena, related to electronically conducting polymers [41, 42]. We recently demonstrated how effective EQCM measurements can be for the study of transport phenomena and adsorption processes related to activated, porous carbon electrodes. It is clear from these studies that EQCM may be an important analytical tool for R&D of electrical double layer capacitor (EDLC) systems [43].

In earlier studies, we used EQCM for selecting ideal electrolyte solutions for rechargeable Li (metal) batteries [38]. We showed that only in solutions based on 1,3 dioxolane (DOL), $LiAsF_6$, and tributyl amine (TBA) as a stabilizer did lithium electrodes behave fully reversibly without any side reactions, due to the formation of unique surface films on Li electrodes in these electrolyte solutions [40]. The m.p.e of Li deposition/dissolution processes in DOL/$LiAsF_6$/TBA solutions measured in EQCM experiments was 7, equal to the equivalent weight of lithium. In parallel, we were able to demonstrate fully reversible behavior of magnesium electrodes in ether solutions (e.g., tetrahydrofuran—THF) comprising complex salts of the $(MgR_2)_x(AlCl_2R')_y$ type (R, R′ are alkyl groups). EQCM measurements of Mg deposition/dissolution processes in these solutions show a m.p.e. of 12, equal to the equivalent weight of magnesium [44].

Another important indication by EQCM measurements that we indeed obtained optimal solutions for Li or Mg batteries was the mass balance upon cycling Li or Mg electrodes in solutions. In appropriate electrolyte solutions

for rechargeable Li and Mg batteries, the mass balance measured was zero in addition to a cycling efficiency close to 100% and m.p.e equal to the equivalent weight for the active metal deposition and dissolution processes.

Diffraction techniques

X-ray diffraction (XRD) is a critically important technique for structural analysis [45]. When light elements are involved (e.g., Li, Mg) and their location in the lattice of compounds is important, neutron diffraction is the right diffractometric technique to use [46]. There is a great deal of very impressive literature on diffractometric data that enables the elucidation of the exact lattice structure for diffractometric measurements using Reitveld analysis [47]. The redox activity of battery materials is usually accompanied by pronounced chemical and structural changes. For example, Li insertion into host materials can involve phase transition or the formation of solid solutions or conversion reactions [48]. In order to understand electrode behavior in Li-ion batteries and to develop new materials, it is critically important to analyze all kinds of structural changes that occur during the course of the electrode's reaction. As ex situ measurements may miss a lot of fine details, it was clear that the use of in situ XRD measurements of Li-insertion electrodes under potential control can provide valuable information. Indeed, in recent decades, many reports on in situ XRD measurements of battery electrodes have been published. Several types of cells were developed in which a Li-insertion electrode is measured exclusively (usually vs. a Li counter electrode), either in the transmittance or reflectance mode, in a way that maximizes the signal-to-noise ratio (minimal interference of other cell components, solution, separator, case, counter electrode, etc.) [49–53]. A very high resolution response can be obtained using an X-ray beam from a synchrotron source [54]. However, there are impressive reports on in situ synchrotron X-ray measurements of Li battery electrodes using regular X-ray diffractometers.

Microscopic techniques

In in situ microscopic techniques, three main tools are relevant: scanning probe microscopy (atomic force and scanning tunneling microscopes—AFM and STM, respectively), scanning electron microscopy (SEM), and tunneling electron microscopy (TEM). AFM and STM are surface sensitive techniques that can be easily modified for in situ microscopic electrochemical measurements [55]. Indeed, since the development of these techniques about 25 years ago, thousands of papers related to their application to electrochemical systems have been published [56, 57]. We were the first to apply AFM for studying in situ Li deposition/dissolution processes [58] and STM for studying ex situ Mg deposition/dissolution processes [59]. These measurements are described in more detail in the next section. Regular SEM and TEM instruments work under high vacuum, and therefore it is impossible to apply such measurements to volatile samples. Consequently, in situ electron microscopic measurements of electrodes submerged in liquid electrolytes are impossible. However, it is definitely possible to construct Li batteries that contain solid electrolyte systems, either polymeric or ceramic, which are non-volatile. In fact, there are reports on in situ TEM and SEM measurements of unique Li-battery systems that are based on solid electrolytes [60, 61]. Highly impressive is a recent report on in situ electron microscopic studies of Li-Sn wire anodes whose changes in the morphology of a single nano Sn fiber are imaged upon its lithiation (an alloying reaction) [62]. There were also attempts to measure cross-sections of Li electrodes during the operation of Li/polymer/electrolyte/Li_xMO_y cells [61].

The development of the so-called environmental SEM instrumentation that works under moderate vacuum, enables the development of in situ SEM electrochemical measurements of electrodes submerged in aqueous solutions. In fact, using environmental SEM, it may be possible to explore in situ morphological changes in electrodes during their electrochemical processes in non-volatile organic or ionic liquid solutions [63].

On the application of selected in situ techniques for the study of Li, Li-graphite, and Mg electrodes

In situ FTIR measurements

Figure 1 shows schematically the main four modes of operation in FTIR spectroscopy: transmittance, reflectance, attenuated total reflectance (ATR), and diffuse reflectance. There are commercial, well-designed accessories for all these modes of operation [64]. For surface studies of adsorbed species, it is recommended to work in the reflectance mode with grazing angles (>80°C) in order to dominate the signals coming from adsorbed species, whose dipole moments are perpendicular to the surface [65]. In addition, it is recommend that S polarized light should be filtered out, thus allowing mostly P polarized light to reach the detector. In this way, it is possible to increase the signal-to-noise ratio related to surface species (which interact better with P polarized light compared to bulk species) [66]. Modern FTIR spectrometers enable kinetic studies by the step-scanning mode [67]. For the ATR mode, IR transparent crystals with a high retractive index are required (>2). Relevant materials are ZnSe, ZnS, Si, and Ge [68]. The beam is directed so as to enter into paralloid or trapezoid

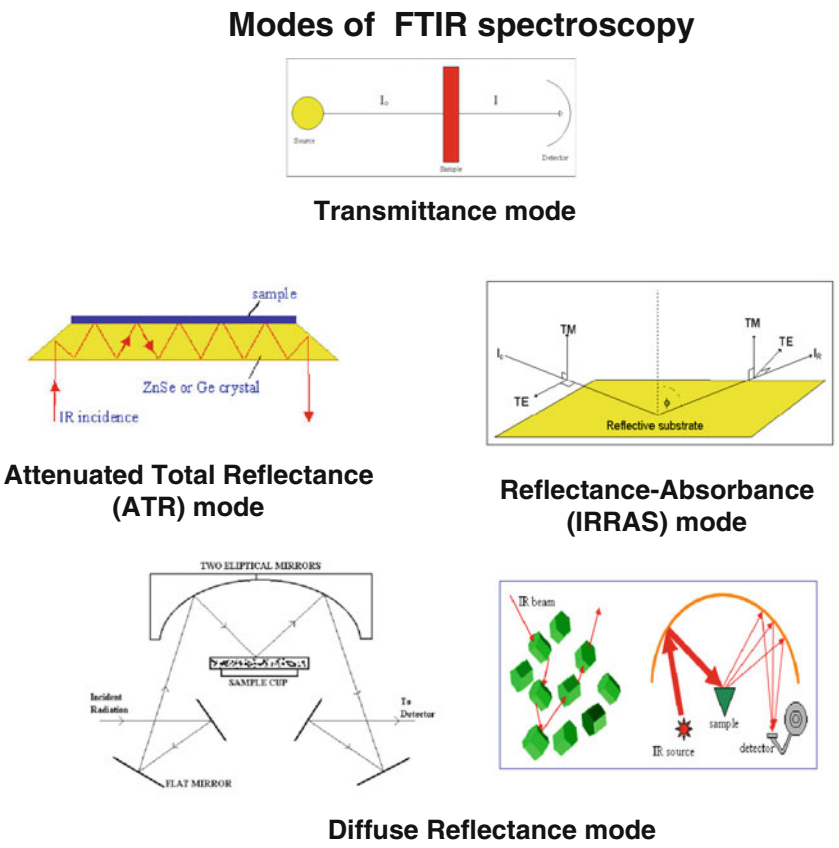

Fig. 1 Typical schemes of various modes of operation in FTIR: transmittance, attenuated total reflectance, reflectance-absorbance and diffuse reflectance [64]

crystals (see Fig. 1) and is internally reflected several times before it leaves the crystal and is directed to the detector. The high refractive index is important to ensure the total internal reflection of the IR beam within the crystal. The IR beam that heats the interface between the crystal and the outside medium has a penetration depth (outside the internal interface) of a half wavelength of relevant light, which for IR beams is in the order of microns. Hence, it is possible to deposit a metallic film on a crystal made of one of the above materials (high refractive index), thus having a working electrode that can be sensed both electrochemically and spectroscopically.

Figure 2 shows schematically three types of cells used for surface studies of highly reactive electrodes by in situ FTIR spectro-electrochemical measurements [69, 70]. We also used the single reflectance mode [71]. Here, the working electrode is a thin film of metal deposited on an optical window of NaCl or KBr. These materials have a low refractive index, but they are transparent to a wide range of wave numbers (600–4,000 cm^{-1} for NaCl and 400–4,000 cm^{-1} for KBr). The beam is directed to the back of the electrodes and is reflected from the internal interface between the working electrode and the optical window, as shown in Fig. 2. This mode of operation allows the use of a relatively cheap optical window and an electrochemical cell design that does not suffer from non-uniform current distribution, as is the case for the thin layer cells required when reflectance modes are used in which the beam has to heat the window and an electrolyte solution layer, (see Fig. 2) on its way to the electrode surface. It should be noted that in order to enhance the signal-to-noise ratio in these types of in situ measurements, modulation techniques were developed. Below we mention two of them:

1. Potential modulation [72]: the electrodes are polarized periodically to the relevant electrochemical reaction potential and back to the open circuit voltage (OCV), and the spectra are collected accordingly. OCV spectra are subtracted from the spectra measured when the electrode was reactive. In such a modulation, it is possible to filter out bulk signals related to interfering solution bands. It should be noted that this mode of operation is relevant if the electrode reactions are fully reversible.
2. Polarization modulation [73]: the polarization of the beam reflected from the electrochemical cell is modulated between the P and S states and the spectra are collected accordingly. Since the P polarized light carries most of the information from the surface species, subtracting the spectra measured at S polarization from those measured at P polarization enables the IR bands of solution bulk to be filtered out, thus

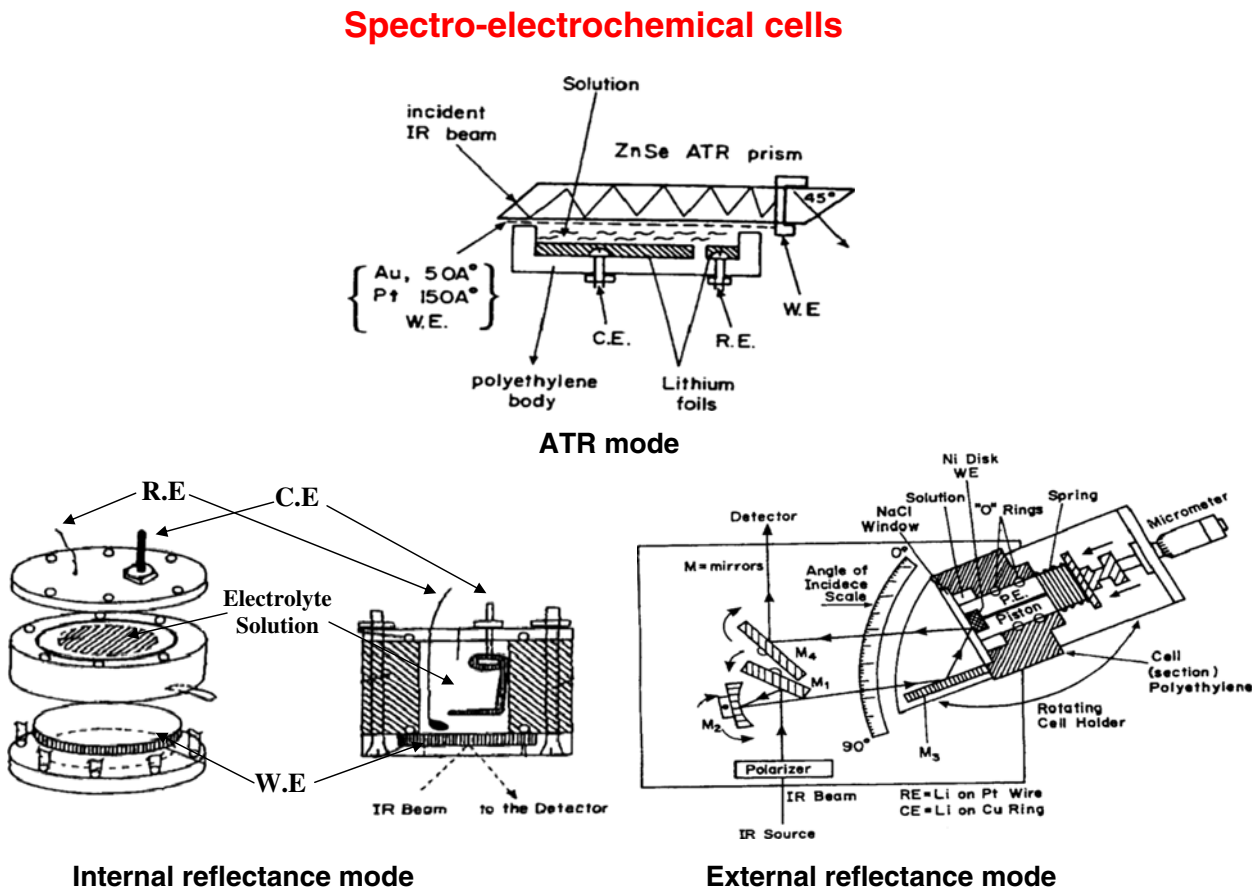

Fig. 2 Cells for three modes of operation for in situ FTIR measurements: ATR, single internal reflectance mode, and external reflectance mode [69–71]

increasing the signal-to-noise ratio of interfacial species. As already reported, the use of in situ FTIR spectroscopy was critically important for resolving the analysis of surface films formed on Li and Li-graphite electrodes in important polar aprotic solutions [69–71]. In ethers, Li electrodes develop surface films comprising ROLi species [74], while in alkyl carbonates Li or Li-C electrodes develop surface films comprising $ROCO_2Li$ species [75]. ROLi species react with both trace H_2O and CO_2, while $ROCO_2Li$ species react with trace H_2O. The final solid product of these reactions is Li_2CO_3. Hence, the use of ex situ spectral measurements may be misleading due to the unavoidable reactions between surface species on active electrodes, and the active electrode material itself, with atmospheric components. Therefore, it can be concluded that only the use of in situ FTIR measurements enabled the analysis of the surface chemistry developed on Li and Li-C electrodes.

As another example of important in situ FTIR measurements of reactive electrochemical systems, Fig. 3 shows a scheme of the cell used (single reflectance mode) and the FTIR spectra obtained during Mg deposition experiments. This process involves the adsorption of Mg-Cl species (that can be part of the mechanism for the deposition process) to be detected during the course of the electrodeposition of magnesium from THF/Mg($AlCl_2EtBu$) complex solutions by the IR measurements [76]. In these solutions, Mg electrodes behave fully reversibly [77] (See structure of the electrolyte in the insert to Fig. 3b, elucidated by single crystal XRD measurements).

As was demonstrated recently, it may be important to conduct in situ FTIR measurements using the transmittance mode. Figures 4a–c show in brief some aspects of such a study, in which the behavior of important ionic liquid solutions was investigated as an electrochemical system with a wide electrochemical window (see the formula of the ionic liquid-based solution (IL) systems, derivatized pyrrolidinium—TFSI in Fig. 4) [78]. Since this IL is non-volatile and its reduction forms gaseous products, it was possible to conduct electrochemical measurements in the cell presented schematically in Fig. 4a, under vacuum. The three-electrode cell is connected to the optical cell with two KBr windows, which contains the gaseous products formed by reactions of the IL solutions. As shown in Fig. 4b, the polarization of graphite electrodes in this IL solution leads to an irreversible process that obviously involves the decompo-

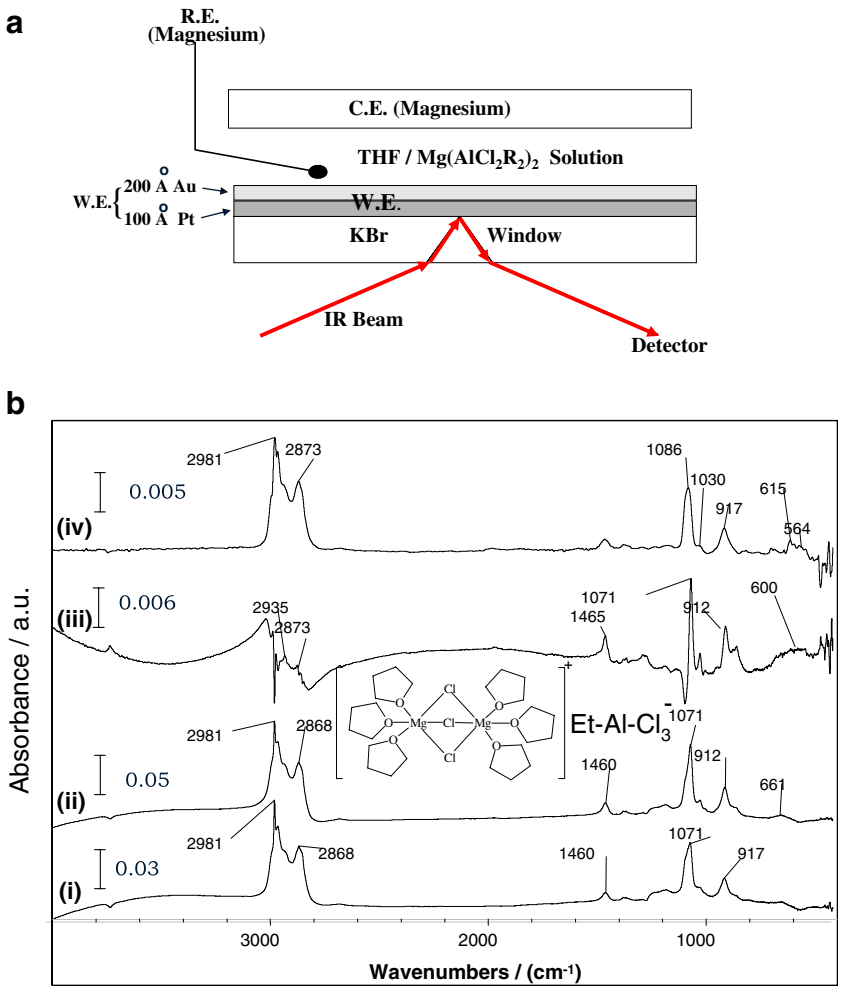

Fig. 3 **a** A Scheme of the spectro-electrochemical cell used for the in situ FTIR measurements (single internal reflectance mode). **b** FTIR spectra obtained from in situ studies of Mg deposition in a THF solution containing the complex salt $MgBu_2{\cdot}(AlCl_2Et)_2$ (Et, Bu = ethyl and butyl groups). (*i*) Measured at OCV before experiment at 2 V vs Mg; (*ii*) measured at 0 V vs Mg after deposition of Mg; (*iii*) subtraction spectrum of (**i**) from (**ii**); (*iv*) a similar spectrum like (**ii**) at 0 V vs Mg but with 0.5 M solution. The insert shows the structure of the electrolyte cation (from a single crystal XRD) [76]

sition of the IL. Indeed, the FTIR spectra measured from this cell upon its cathodic polarization (see Fig. 4c) do show peaks of R_3N species and C_2H_4 evolved during the cation reduction and CHF_3 from the anion reduction. These measurements allowed, for the first time, an understanding of the cathodic reactions of these IL solutions that limit their electrochemical window. We should acknowledge the intensive studies of the effect of reactive additives on electrolyte solutions for Li-ion batteries in which in situ FTIR measurements were used [79–82]. In these studies, an external reflectance mode was used in which the IR beam is reflected from the working electrode (inert metal polarized to low potentials), crossing twice the optical window and a thin solution layer (see Fig. 2). We should also mention our own study of in situ FTIR measurements in which a single internal reflectance mode was used for understanding the oxidation processes of alkyl carbonate solutions [83].

In situ Raman measurements

In situ Raman measurements for the analysis of electrochemical systems have been used for more than three decades [84]. Raman measurements are also highly important for the analysis of both electrode materials and electrolyte solutions of battery systems, and, in fact, there is no serious study in the field that does not use Raman spectroscopy as an important analytical tool. In recent years, we have seen an increasing number of publications reporting on in situ Raman measurements related to battery material. In this paper, we mention a typical study related to the behavior of graphite electrodes in ionic liquid-based solutions [85, 86]. This is an important topic because the use of ILs in Li-ion batteries can be beneficial for their safety and the possibility of using high-voltage cathode materials (i.e., elaborating high energy density batteries) due to the very wide electrochemical window of many ILs [87].

Modern micro-Raman spectrometers available today enable measurements of several points on an electrode surface. Thus, it is possible to confirm that the spectral data are really representative. Figure 5a and b shows the scheme of the cell and formula of the ionic liquid, a derivatives of piperidinium cation with a $(CF_3SO_2)_2N^-$ (TFSI) anion that we used in our study. Figure 5b shows three consecutive

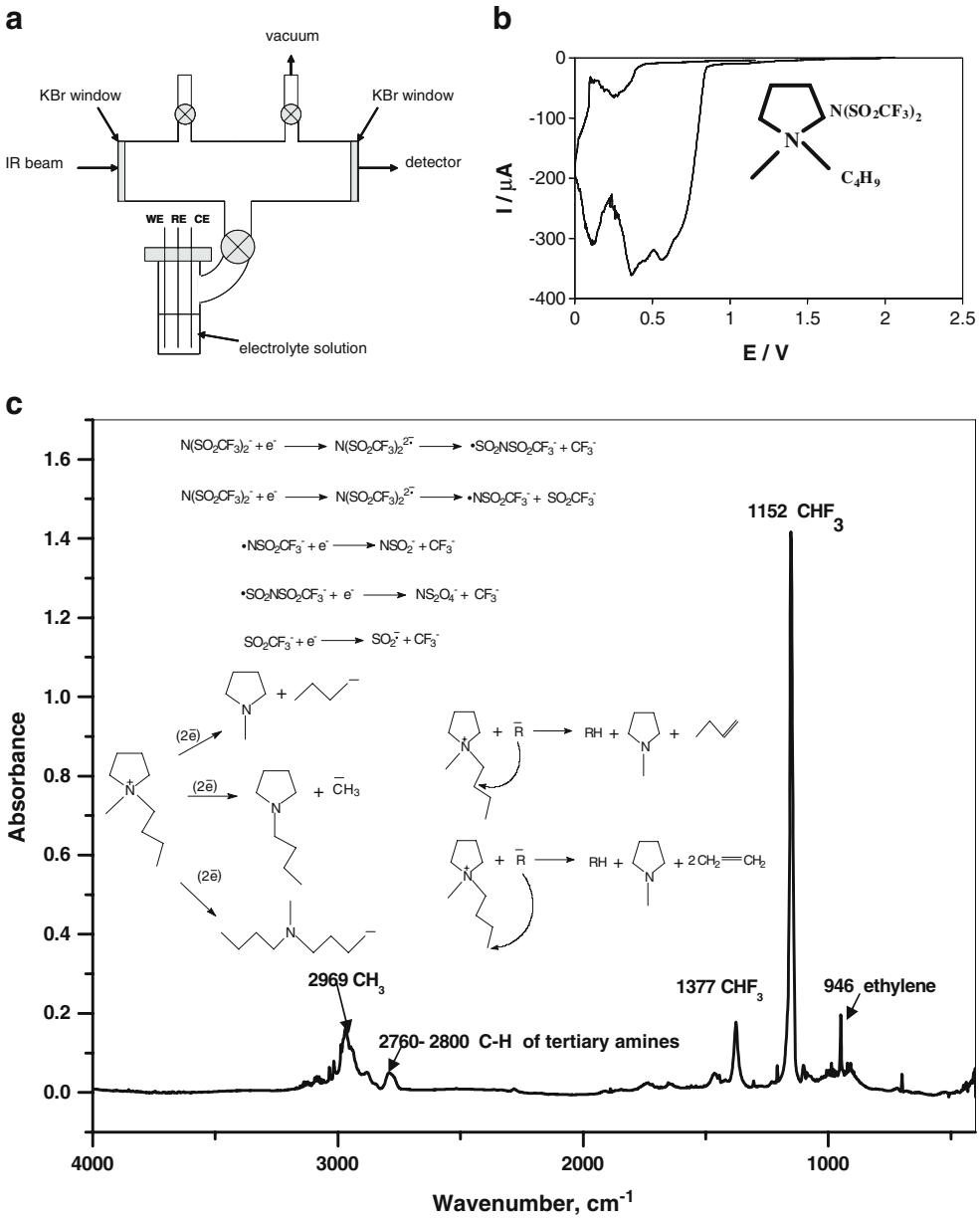

Fig. 4 **a** A cell for in situ FTIR measurements in transmittance mode attached to an electrochemical cell for work with ionic liquids under vacuum. **b** A typical first cycle voltammogram of a graphite electrode in the pyrrolidinium-TFSI/LiTFSI solution (see structural formula in the *inset*). This voltammogram reflects fully irreversible behavior. **c** A typical FTIR spectrum obtained upon the polarization of the graphite electrode in the IL solution in the cell of (**a**). Peak assignments appear therein [78]

cyclic voltammograms (CVs) of a composite graphite electrode comprising synthetic graphite flakes as the active mass. These three CVs show a pair of peak at 0.3–0.5 V vs. Li/Li^+ (cathodic) and 1 V (anodic) and a pair of peaks around 0 V (cathodic) and 0.3 V (anodic).

Figure 6 shows the Raman spectra measured in situ from this specific electrode during the course of cathodic and anodic potential scanning in the second CV cycle. As marked in this figure, there are distinctive Raman peaks related to lithiated graphite and to graphite intercalated with the piperidinium cation of the IL [85, 86]. Hence, we can conclude from these measurements that the co-intercalation of the IL cation interferes with reversible Li insertion into graphite in this IL solution. It takes several CV cycles to passivate the electrode by the reduction products of the TFSI anion [85, 86]. Thus, the peaks related to the intercalation of the IL cation into graphite go down from cycle to cycle (Fig. 5b) because the passivating surface films thus formed allow only Li-ion transport to the graphite particles from the solution phase, and screen out the transport of the IL cations to the active mass. This study is a typical example in which in situ spectroscopic studies enabled an understanding of the electrochemical responses (the data in Fig. 6 explain what is seen in Fig. 5b).

In situ scanning probe microscopic measurements (AFM and STM)

As mentioned above, in situ AFM and STM measurements of electrochemical systems are widely used, and every

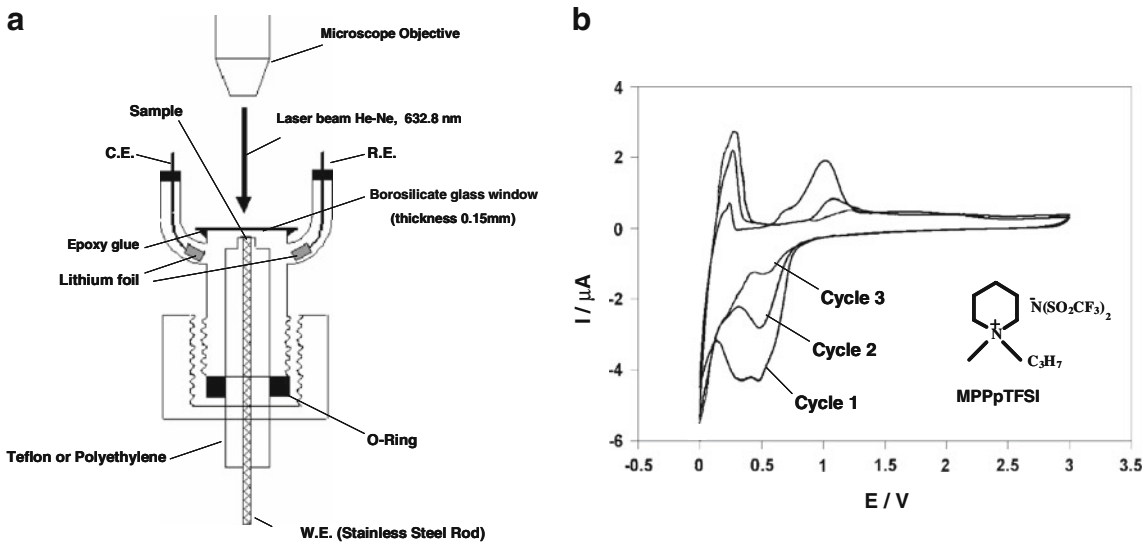

Fig. 5 **a** A cell for the in situ Raman measurements. **b** Typical consecutive cyclic voltammograms of a graphite electrode comprising synthetic flakes in the piperidinium-TFSI/LiTFSI solution (see structural formula therein) [85, 86]

month there are several dozens of new publications on these topics. In recent years, AFM measurements were very elegantly used to demonstrate volume changes upon the reversible lithiation of the tin electrodes [88–90] and morphological studies of carbon electrodes [91, 92]. We provide herein three classic examples of the use of AFM and STM for in situ studies of the most reactive electrochemical systems. A special work station was developed and built for these measurements, as was already described in detail [93]. These include evacuable glove boxes in which the microscopes are placed, and enable work under a highly pure argon atmosphere. These evacuable glove boxes are hung from the ceiling by flexible bungee cords that fully protect them from vibrations. Special spectro-electrochemical cells were developed that allow work with volatile organic solutions. In addition, a special system was developed for preparing tips for STM measurements in polar aprotic organic solutions (most of the tip, except for its sharp edge, has to be covered by an insulating polymeric layer that does not dissolve in the

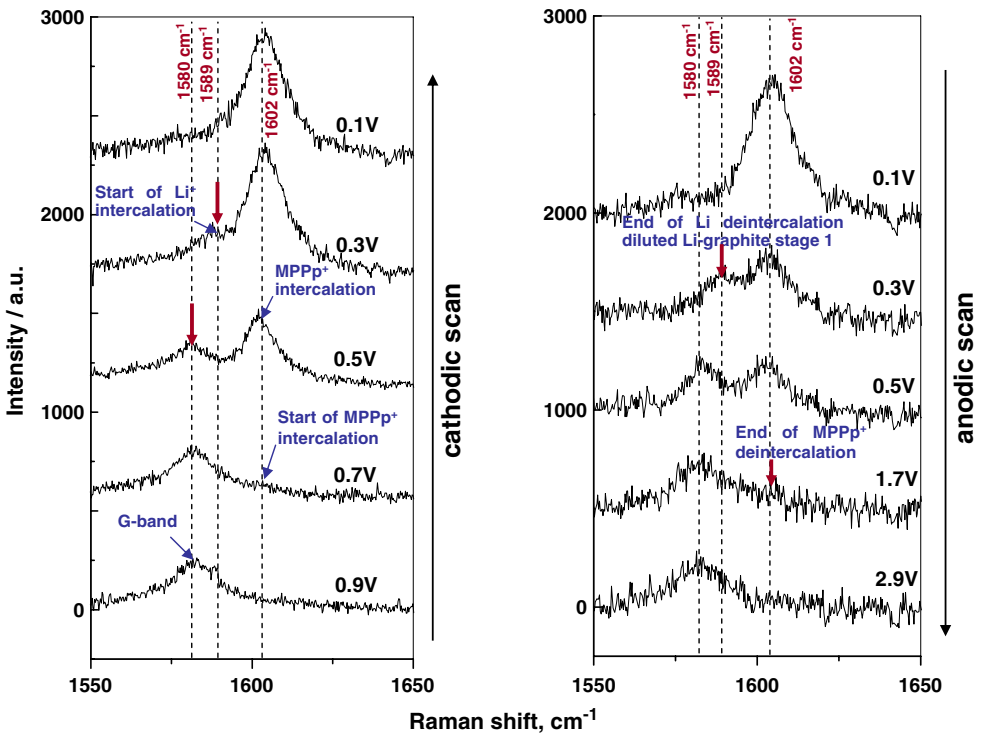

Fig. 6 Typical Raman spectra measured in situ from the graphite electrode whose CVs are presented in Fig. 5b upon cathodic and anodic potential scans, as indicated, peak assignments are presented therein [85, 86]

organic solvents, in order to ensure the flow of a tunneling current through the tip) [93].

Figure 7 shows typical AFM images of an area in a Li electrode in an ethylene carbonate and di-methyl carbonate (EC-DMC)/$LiPF_6$ solution that is undergoing electrochemical dissolution [94]. Since the surface films on the active metal through which Li ions have to migrate are very non-uniform, there are points of high current density in which Li dissolution and the related morphological changes are very pronounced. The surface films are not flexible enough to accommodate such changes; they are broken down, which exposes a fresh Li surface for solution species. Fast reactions between the freshly exposed lithium and solution components form surface species that repair the broken surface films, i.e., Li is dissolved via a break-and-repair mechanisms of the surface films. The scheme in Fig. 7 explains clearly the findings by in situ AFM measurements.

Figure 8 shows AFM images of a Li electrode in the same solutions that undergoes Li deposition processes [95]. It also includes a picture measured by a CCD camera of the AFM system and a scheme that explains what is seen. The non-uniformity of the surface films forms points of high current density due to local low resistivity of the surface films to Li-ion migration under the electrical field. Li dendrites thus emerge from the surface films and immediately react with solution species. The CCD camera captured nicely the growth of Li dendrites (millimeter size) as the cathodic process continues. The AFM measurements were able to image very well the events at the beginning of the dendrite formation. It should be noted that dendrite formation upon metal deposition processes can be considered as an auto-catalytic process. This entire process is explained by the scheme in Fig. 7 (upper part). It should be noted that dendrite formation is the major failure process of Li electrodes and which led to their replacement by Li-graphite anodes in rechargeable Li-ion batteries. The left illustration in both schemes in Figs. 7 and 8 show a hypothetic situation in which the surface films are flexible enough to accommodate morphological changes of Li electrodes upon intensive Li deposition or dissolution.

Figure 9 presents AFM images obtained in situ with graphite electrodes upon their polarization in two types of

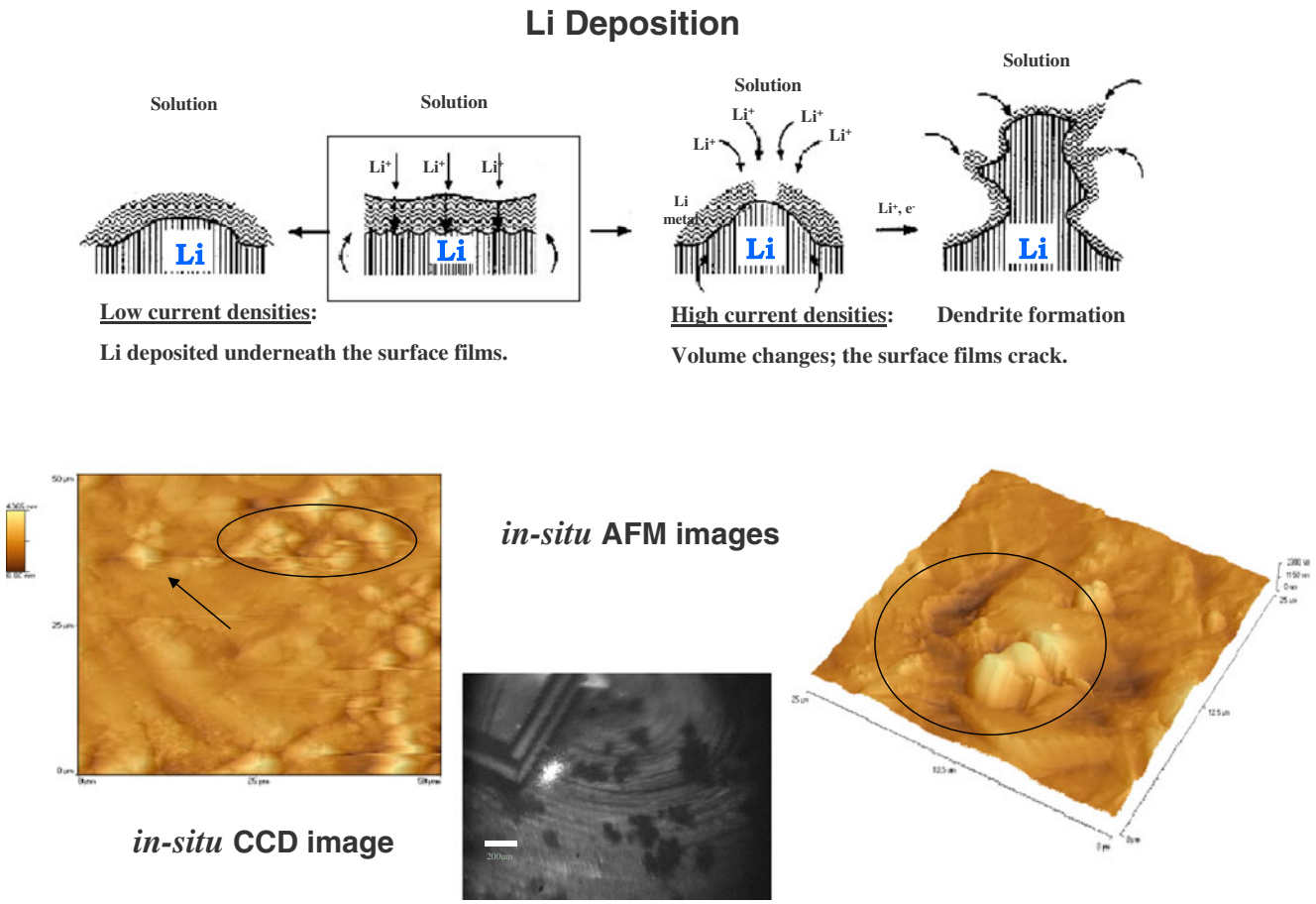

Fig. 7 Typical AFM images obtained in situ from Li electrodes polarized anodically in EC-DMC/$LiPF_6$ solutions that show the break-and-repair of the surface films during the course of Li dissolution. The scheme above explains the situation on the Li surfaces. The left chart presents a hypothetical situation in which the surface films are flexible and accommodate the Li morphological changes [94]

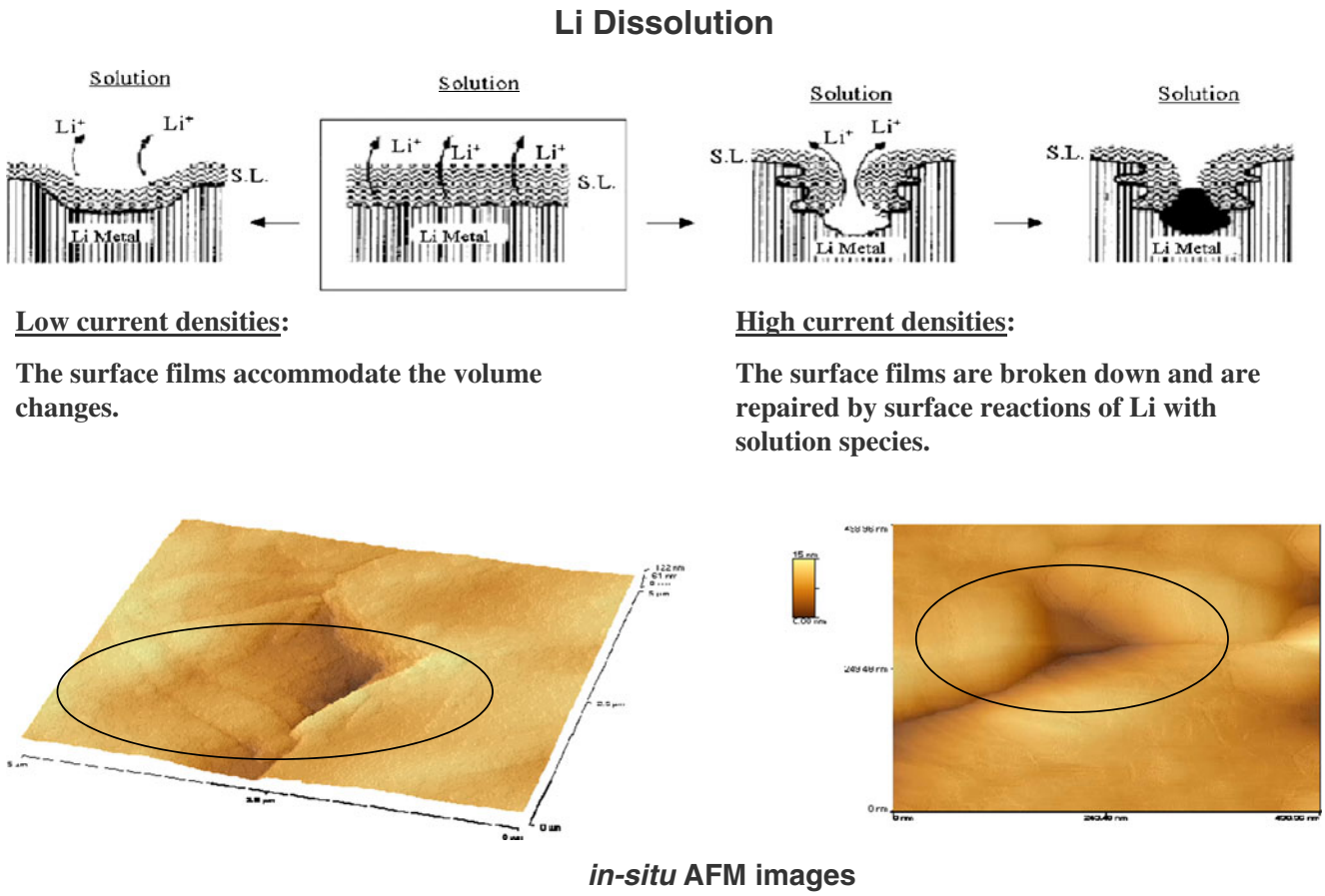

Fig. 8 Typical AFM images obtained in situ from Li electrodes polarized cathodically in EC-DMC/$LiPF_6$ solutions that show the beginning of dendrite formation. In the lower part of the figure, a picture taken with a CCD camera attached to the AFM system is presented, showing the growth of dendrites as Li deposition proceeds. The scheme in the upper part of the figure explains the images, showing schematically how dendrites are formed due to non-uniform current distribution [95]

electrolyte solutions [96, 97]. These images were measured during the course of the cathodic polarization of graphite electrodes. In solutions based on EC-DMC mixtures with any Li salt (e.g., $LiAsF_6$, $LiPF_6$, $LiClO_4$, $LiN(SO_2CF_3)_2$), cathodic polarization leads to a fast reduction of EC at potential below 1.2 V (e.g., $EC + 2e^- + 2Li^+ \rightarrow (CH_2OCO_2Li)_2 \downarrow + C_2H_4 \uparrow$) [98]. The reaction products of EC precipitate on the graphite surface as compact Li ions conducting but electronic insulating, passivating surface films [99]. Such films avoid the co-intercalation of solvent molecules together with Li ions and the destruction of the graphite structure (e.g., by its exfoliation due to the reduction of co-intercalated solvent molecules within the graphite bulk). Indeed, AFM images of graphite electrodes in such solutions (see Fig. 9, upper part) reflect stability in which no visible morphological changes has been observed upon cycling during in situ AFM measurements [96].

In contrast, when the electrolyte solution contains a component such as propylene carbonate (PC), we obtain bad passivation of cathodically polarized graphitized mesocarbon microbead (MCMB) electrodes. Hence, PC molecules are co-intercalated with Li^+ ions, reduced therein, and the graphite particles crack, as so clearly imaged by in situ AFM measurements [97]. Hence, this type of in situ morphological study enabled an understanding of the main failure mechanisms of graphite electrodes in Li salt solutions. Note that studies of techniques such as SEM and XRD could not be conclusive about the "cracking" of graphite particles as one of the major failure mechanisms of graphite electrodes.

Finally, we provide herein an example of the use of in situ STM measurements for the study of Mg deposition [100]. The possibility of using STM measurements for such studies is significant in itself because it means that Mg deposition and reversible Mg electrodes relate only to a surface film/passivation-free situation. When Mg electrodes or metallic substrates in Mg ions containing solutions are passivated, there is no way to obtain electrochemical Mg deposition because surface films comprising ionic Mg compounds (Mg salts) are completely blocking for Mg ion transport [101]. Mg electrodes can behave fully reversibly in ethereal solutions

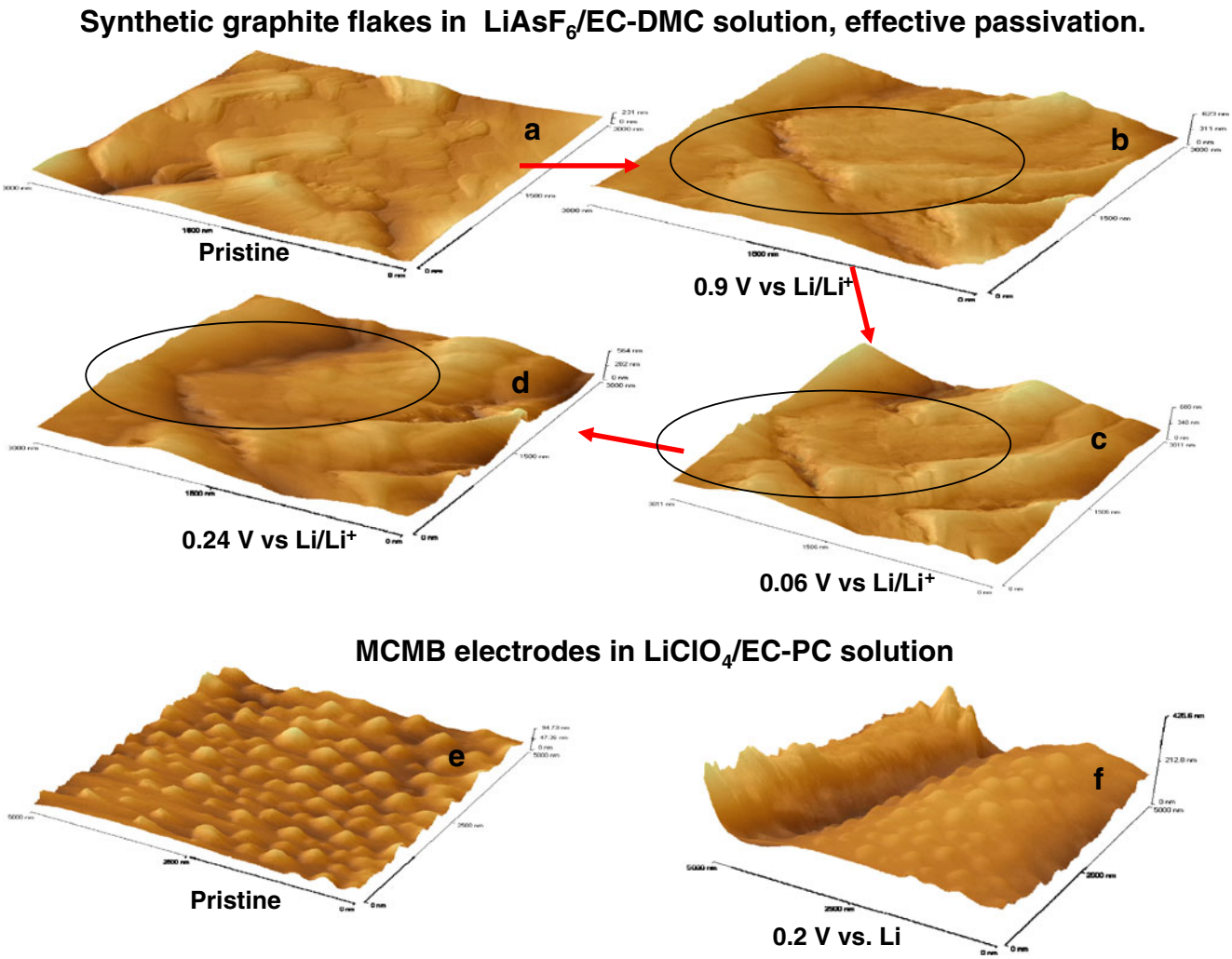

Fig. 9 AFM images measured in situ with two types of graphite electrodes in two different solutions, during their cathodic polarization. *Upper part* an electrode comprising graphite flakes in EC-DMC/1 M $LiAsF_6$ solutions, stable situation [96]. *Lower part* an electrode comprising mesocarbon microbead (*MCMB*) particles in a EC:PC/$LiClO_4$ solution. The graphite particles crack due to the poor passivation and reduction of co-intercalated solvent molecules within the graphite bulk. The potential at which the images were measured are marked therein [97]

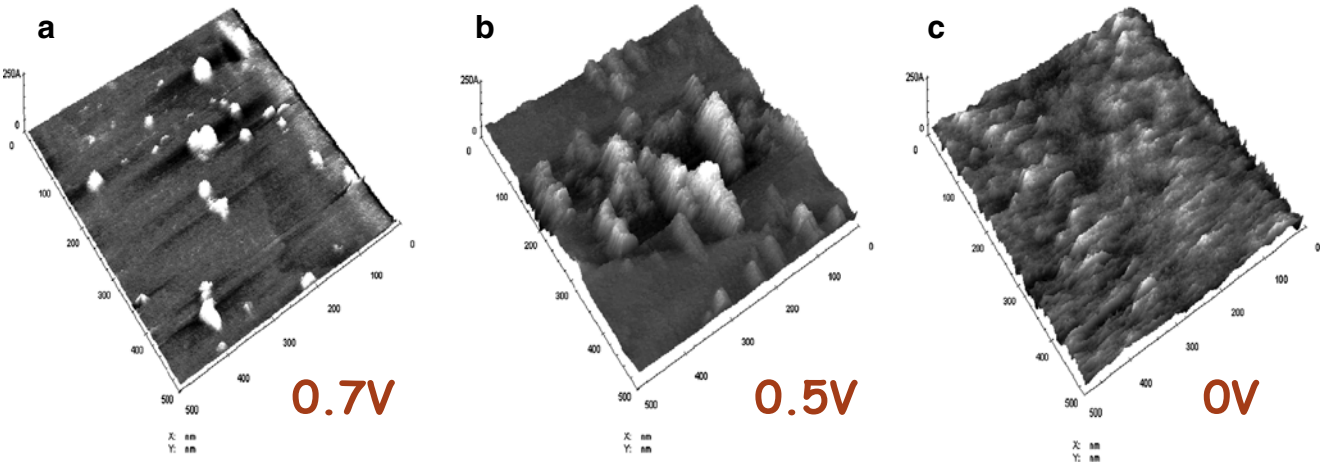

Fig. 10 STM images of gold electrodes polarized cathodically in a tetra glyme, CH_3O-(CH_2CH_2O-)CH_3/$MgBu_2$-($AlCl_2Et$)$_2$ 0.25 M solution (Bu, Et = butyl and ethyl group). The relevant potentials are marked therein. An image measured at 0 V after Mg deposition is also presented [100]

containing complex salts of the RMgX or $Mg(AX_{4n}R_n)_2$ type, where R = alkyl or aryl group, A = an element such as Al or B, and X = halides such as Cl^- or Br^-). It was important to discover that even "heavy" ethers such as tetra glyme, TG (CH_3-O(CH_2CH_2-O)$_4$-CH_3), can be used [102].

Figure 10 shows STM images of gold electrodes polarized in TG solutions containing a similar salt Bu_2Mg-$(AlEtCl_2)_2$ (Bu = butyl, Et = ethyl group). This electrolyte solution may be important for rechargeable Mg batteries because this ether solvent is not volatile, thus having good safety features. Electrochemical measurements of Mg or noble metal electrodes in these solutions demonstrated highly reversible Mg deposition/dissolution behavior [102]. STM images measured in situ during the course of cathodic polarization of inert electrodes in this electrolyte solution showed the formation of sporadic, nanometer size surface adsorbed species (see Fig. 10) that do not interfere badly with the possibility of imaging the electrode's surface by STM and with further Mg deposition at the potential set below 0 V vs. Mg. The STM imaging experiments with all ether-complex solutions correlated well with in situ FTIR measurements (see above discussion, related to Fig. 4) that indicate the adsorption of Mg-Cl species at low potentials. Rigorous electrochemical studies of Mg deposition reactions with microelectrodes [15] also showed that the mechanism of Mg deposition in the ethereal-complex salt solutions discussed herein includes the critical steps of cation adsorption (Mg-Cl species, see insert to Fig. 4). Hence, it appears that the in situ STM measurements of Mg deposition do image the electro-adsorption steps that precede the deposition process.

Conclusion

Most of the analytical tools used in materials science, spectroscopic (FTIR, Raman, MS, and NMR), diffractometric (by X-ray or neutrons), microscopic (SEM, TEM, AFM, and STM), and synchrotron X-ray-based techniques (XANES and EXAFS) can be applied to electrochemical systems as in situ measurements in which the analysis is made while the systems are maintained under potential control. In work related to R&D of batteries, the use of in situ techniques may be very important because battery electrode materials may be highly reactive due to the requirement for high energy density of battery systems. The analysis of active battery materials may be intensively interfered with by reactions of these materials with atmospheric components. Hence, spectroscopic or microscopic studies of such materials by ex situ measurements may not be authentic. The materials thus measured may change their surface chemistry, and even bulk properties, on the way from the electrochemical cell to the analytical system.

In this review, we specifically selected examples related to four techniques: FTIR and Raman spectroscopies and AFM and STM in situ studies of Li, Li-graphite, and magnesium electrodes. We tried to demonstrate the uniqueness of such measurements, applied to highly reactive electrochemical systems, and the specific information gained from the fact that the measurements are carried out while the electrodes are in solutions, under potential control.

References

1. Odziemkowski M, Irish DE (1992) J Electrochem Soc 139:3063
2. Lu Z, Schechter A, Moshkovich M, Aurbach D (1999) J Electroanal Chem 466:203
3. Gendersa JD, Pletcher D (1986) J Electroanal Chem Interfacial Electrochem 199:93
4. Peled E (1983) In: Gabano JP (ed) Lithium Batteries. Academic, London
5. Peled E (1979) J Electrochem Soc 126:2047
6. Aurbach D, Zinigrad E, Teller Y, Cohen Y, Salitra G (2002) J Electrochem Soc 149:A1267
7. Yamaki J-i, Tobishima S-i, Hayashi K, Saito K, Nemoto Y, Arakawa M (1998) J Power Sources 74:219
8. Abraham KM (1993) Electro chimica Acta 38:1233
9. Aurbach D, Moshkovich M, Gofer Y (2001) J Electrochem Soc 148:E155
10. Aurbach D, Moshkovich M, Cohen Y, Schechter A (1999) Langmuir 15:2947
11. Winter M, Besenhard JO, Spahr ME, Novák P (1998) Adv Mater 10:725
12. Verma P, Maire P, Novák P (2010) Electrochim Acta 55:6332
13. Aurbach D, Markovsky B, Salitra G, Markevich E, Talyossef Y, Koltypin M, Nazar L, Ellis B, Kovacheva D (2007) J Power Sources 165:491
14. Gregory TD, Hoffman RJ, Winterton RC (1990) J Electrochem Soc 137:775
15. Viestfried Y, Levi MD, Gofer Y, Aurbach D (2005) J Electroanal Chem 576:183
16. Ostrovskii D, Ronci F, Scrosati B, Jacobsson P (2001) J Power Sources 103:10
17. Dokko K, Mohamedi M, Anzue N, Itoh T, Uchida I (2002) J Mater Chem 12:3688
18. Grey CP, Dupre N (2004) Chem Rev 104:4493
19. Gireaud L, Grugeon S, Pilard S, Guenot P, Tarascon J-M, Laruelle S (2006) Anal Chem 78:3688
20. Totir DA, Bae IT, Hu Y, Antonio MR, Stan MA, Scherson DA (1997) J Phys Chem B 101:9751
21. Fleischmann M, Hendra PJ, MacQuillan A (1974) Chem Phys Lett 26:163
22. Grey CP, Lee YJ (2003) Solid State Sci 5:883
23. Lee YJ, Wang F, Grey CP (1998) J Am Chem Soc 120:12601
24. Laws DD, Bitter H-ML, Jerschow A (2002) Angew Chem Int Ed 41:3096
25. Key B, Bhattacharyya R, Morcrette M, Sezne V, Tarascon J-M, Grey CP (2009) J Am Chem Soc 131:9239
26. Imhof R, Novák P (1999) J Electrochem Soc 146:1702
27. Lanz M, Novák P (2001) J Power Sources 102:277
28. Kim J-M, Chung H-T (2004) Electrochim Acta 49:937
29. Deba A, Cairns EJ (2006) Fluid Phase Equilib 241:4

30. Ota H, Akai T, Namita H, Yamaguchi S, Nomura M (2003) J Power Sources 119:567
31. Nakai I, Nakagome T (1998) Electrochem Solid State Lett 1:259
32. Deb A, Bergmann U, Cairns EJ, Cramer SP (2004) J Synchrotron Rad 11:497
33. Xie Q, Li Z, Deng C, Liu M, Zhang Y, Ma M, Xia S, Xiao X, Yin D, Yao S (2007) J Chem Educ 84:681
34. Morita M, Ichimura T, Ishikawa M, Matsuda Y (1997) J Power Sources 68:253
35. Barisci JN, Wallace GG, Baughman R (2000) Electrochim Acta 46:509
36. Shackleford SGD, Boxall C, Port SN, Taylor RJ (2002) J Electroanal Chem 538:109
37. Hepel M, Xingmin Z, Stephenson R, Perkins S (1997) Microchem J 56:79
38. Aurbach D, Zaban A (1995) J Electrochem Soc 142:L108
39. Lei H-W, Uchida H, Watanabe M (1996) J Electroanal Chem Interfacial Electrochem 413:131
40. Aurbach D, Moshkovich M (1998) J Electrochem Soc 145:2629
41. Chung S-M, Paik W-k, Yeo I-H (1997) Synth Met 84:155
42. Cohen YS, Levi MD, Aurbach D (2003) Langmuir 19(23):9804
43. Aurbach D, Levi M, Salitra G, Maier J (2009) Nat Mater 8:872
44. Aurbach D, Gofer Y, Schechter A, Chusid O, Gizbar H, Cohen Y, Moshkovich M, Turgeman R (2001) J Power Sources 97:269
45. Harris KDM, Tremayne M (1996) Chem Mater 8:2554
46. Mitelman, Levi E, Isnard E, Aurbach D (2007) J Inorg Chem 46:7528
47. Will G (2006) Powder diffraction. Springer, Berlin
48. Tarascon J-M, Armand M (2001) Nature 414:359
49. Aurbach D, Eli YE (1995) J Electrochem Soc 142:1746
50. Aurbach D, Levi E, Levi MD, Salita G, Markovsky B, Gamolsky K, Oesten R, Heider U, Heider L (1999) Solid State Ionics 126:97
51. Yoona W-S, N Kima X-QY, McBreenb J, Grey CP (2003) J Power Sources 119:649
52. Courtney IA, Dahn JR (1997) J Electrochem Soc 144:2045
53. Reimers JN, Dahn JR (1992) J Electrochem Soc 139:2091
54. Alcántara R, Jaraba M, Lavela P, Tirado JL (2003) Chem Mater 15:1210
55. Magonov SN, Whangbo M-H (1996) Surface analysis with STM and AFM. VCH-Weinheim, New York
56. Davis JJ, Hill HAO, Bond AM (2000) Coord Chem Rev 200:411
57. Li Y, Maynor BW, Liu J (2001) J Am Chem Soc 123:2105
58. Aurbach D, Cohen Y (1997) J Electrochem Soc 144:3355
59. Aurbach D, Cohen Y, Moshkovich M (2001) Electrochem Solid State Lett 4:A113
60. Dollé M, Sannier L, Beaudoin B, Trentin M, Tarascon J-M (2002) Electrochem Solid State Lett 5:A286
61. Orsini F, Pasquier AD, Beaudoin B, Tarascon JM, Trentin M, Langenhuizen N, Beer ED, Notten P (1998) J Power Sources 76:19
62. Ying Z, Wana Q, Cao H, Song ZT, Feng SL (2005) Appl Phys Lett 87:113108
63. Xu F, Jung C (2010) J Electrochem Soc Meet Abstr 108:1003
64. Griffiths PR, Haseth JAD (2007) Fourier transform infrared spectrometry, 2nd edn. Wiley-Interscience, New York
65. Surca A, Orel B, PIHLAR B (1997) J Sol Gel Sci Technol 8:743
66. Kanamura K, Umegaki T, Ohashi M, Toriyama S, Shiraishi S, Takeharad Z-i (2001) Electrochim Acta 47:433
67. Zhou Z-Y, Lin S-C, Chen S-P, Sun S-G (2005) Electrochem Commun 7:490
68. Song S-W, Zhuang GV, Ross PN Jr (2004) J Electrochem Soc 151:A1162
69. Goren E, Chusid O, Aurbach D (1991) J Electrochem Soc 138: L6
70. Aurbach D, Chusid O (1993) J Electrochem Soc 140:L155
71. Chusid O, Aurbach D (1993) J Electrochem Soc 140:L1
72. Matsui M, Dokko K, Kanamura K (2010) J Electrochem Soc 157:A121
73. Barusseau S, Beden B, Broussely M, Perton F (1995) J Power Sources 54:296
74. Aurbach D, Granot E (1997) Electrochim Acta 42:697
75. Marom R, Halalay I, Haik O, Zinigrad E, Aurbach D (2010) J Electrochem Soc 157:A972
76. Aurbach D, Turgeman R, Chusid O, Gofer Y (2001) Electrochem Commun 3:252
77. Aurbach D, Gizbar H, Schechter A, Chusid O, Gottlieb HE, Gofer Y, Goldberg I (2002) J Electrochem Soc 149:A115
78. Markevich E, Sharaby R, Burgel V, Semrau G, Schmidt M, Aurbach D (2010) Electrochim Acta 55:2687
79. Santner HJ, Korepp C, Winter M, Besenhard JO, Moller K-C (2004) Anal Bioanal Chem 379:266
80. Balducci A, Schmuck M, Kern W, Rupp B, Passerini S, Winter M (2008) ECS Trans 11:109
81. Korepp C, Santner HJ, Fujii T, Ue M, Besenhar JO, Möller K-C, Winter M (2006) J Power Sources 158:578
82. Korepp C, Kern W, Lanzer EA, Raimann PR, Besenhard JO, Yang M, Möller K-C, Shieh D-T, Winter M (2007) J Power Sources 174:628
83. Moshkovich M, Cojocaru M, Gottlieb HE, Aurbach D (2001) J Electroanal Chem 497:84
84. Hadjean RB, Ramos J-PP (2010) Chem Rev 110:1278
85. Markevich E, Baranchugov V, Salitra G, Aurbach D (2008) J Electrochem Soc 155:A132
86. Baranchugov V, Markevich E, Salitra G, Schmidt M, Aurbach D (2008) J Electrochem Soc 155:A217
87. Lewandowski A, S'widerska-Mocek A (2009) J Power Sources 194:601
88. Tian Y, Timmons A, Dahn JR (2009) J Electrochem Soc 156: A187
89. Beaulieu LY, Beattie SD, Hatchard TD, Dahn JR (2003) J Electrochem Soc 150:A419
90. Beaulieu LY, Hatchard TD, Bonakdarpour A, Fleischauer MD, Dahn JR (2003) J Electrochem Soc 150:A1457
91. Campana FP, Kötz R, Vetter J, Novák P, Siegenthaler H (2005) Electrochem Commun 7:107
92. Alliata D, Häring P, Haas O, Kötz R, Siegenthaler H (1999) Electrochem Commun 1:5
93. Cohen Y, Aurbach D (1999) Rev Sci Instrum 70:4668
94. Aurbach D, Cohen Y (1999) Electrochem Solid State Lett 2:16
95. Aurbach D, Cohen Y (2000) J Phys Chem B 104:12282
96. Koltypin M, Cohen Y, Markovsky B, Aurbach D (2002) Electrochem Comm 4:17
97. Aurbach D, Koltypin M, Teller H (2002) Langmuir 18:9000
98. Aurbach D, Levi MD, Levi E, Schechter A (1997) J Phys Chem B 101:2195
99. Aurbach D, Gnanaraj JS, Levi MD, Levi E, Salitra G, Fischer JF, Claye A (2001) J Electrochem Soc 148:A525
100. Aurbach D, Schechter A, Moshkovich M, Cohen Y (2001) J Electrochem Soc 148:A1004
101. Aurbach D, Zhongua L, Schechter A, Gofer Y, Gizbar H, Turgeman R, Cohen Y, Moshkovich M, Levi E (2001) J Power Sources 97:28
102. Aurbach D, Weissman I, Gofer Y, Levi E (2003) Chem Rec 3:61